

Renormalization Group Approach to Anderson Impurity in the Bulk of Topological Insulators

Igor Kuzmenko¹, Yshai Avishai^{1,2} and Tai Kai Ng²

¹*Department of Physics, Ben-Gurion University of the Negev Beer-Sheva, Israel*

²*Department of Physics, Hong Kong University of Science and Technology, Kowloon, Hong Kong*
(Dated: March 6, 2013)

It has been recently suggested that when an Anderson impurity is immersed in the bulk of a topological insulator, a Kondo resonant peak will appear simultaneously with an in-gap bound-state when the band-dispersion has an "inverted-Mexican-hat" form. The mid-gap bound-state generates another spin state and the Kondo effect is thereby screened. In this paper we study this problem within a weak-coupling RG scheme where we show that the system exhibits complex crossover behavior between different symmetry configurations and may evolve into a self-screened-Kondo or $SO(3)$ low energy fix point. Experimental consequences of this scenario are pointed out.

Introduction

The significance of topological insulators as a new state of matter has been stressed in numerous publications [1–7]. So far, the main attention on the physics in topological insulators has been focused on the surface states [9–22]. It was pointed out recently that impurity scattering may have non-trivial effects in the *bulk* of TI due to its particular band structure [23–25]. For topological non-trivial insulators with "inverted-Mexican-hat" band dispersion around the Γ -point, in-gap bound states are induced by impurities with arbitrary weak scattering [23]. The presence of the in-gap bound state affects profoundly the Kondo physics associated with magnetic impurities in the bulk of topological insulators. Using a slave-boson mean-field theory [24], it was shown that the Kondo resonance could be screened by the exchange interaction $\sim J_{df} \mathbf{S}_d \cdot \mathbf{S}_f$ (with $J_{df} > 0$) between the spins of the Kondo (d) impurity and the induced bound-state (f), leading to a self-screened Kondo effect [24].

The physics described above is not limited to topological insulators but is a general consequence of insulators (and semi-conductors) with a large electronic density of states at the band edge such that in-gap bound states are easily induced by an Anderson impurity. The goal of this work is to perform a detailed analysis of the interplay between the Anderson impurity and its induced in-gap bound state. Using a weak-coupling renormalization group (RG) analysis, we show that the system exhibits complex crossover behavior between different symmetry sectors and that the exchange interaction J_{df} between the d - and f -spins may be renormalized dynamically to a negative value at suitable parameters regime. In this case the Kondo effect is not screened and the low energy physics of the system is described by an $SO(3)$ Kondo fix point. The temperature dependence of the impurity induced resistance and magnetic susceptibility are studied at various regimes.

Model

We consider an Anderson impurity d in the bulk of an insulator. For concreteness we shall consider the Hamiltonian of a two-dimensional topological insulator (2DTI) $H = H_0 + H_d + H_t + V$ [24], where H_0 describes electrons in the bulk of the TI,

$$H_0 = \hbar v_F (\mathbf{k} \cdot \boldsymbol{\alpha}) + \beta \{ m v_F^2 - B \hbar^2 k^2 \}, \quad (1a)$$

with $\boldsymbol{\alpha} = t_x \otimes \mathbf{s}$ and $\beta = t_z \otimes s_0$, where $\mathbf{t} = (t_x, t_y, t_z)$ or $\mathbf{s} = (s_x, s_y, s_z)$ are vectors of the Pauli matrices acting in the space of isospins or spins, s_0 is the 2×2 identity matrix. The basis vectors are chosen as

$$\Psi_{\mathbf{k}} = \begin{pmatrix} a_{\mathbf{k}\uparrow} \\ a_{\mathbf{k}\downarrow} \\ b_{\mathbf{k}\uparrow} \\ b_{\mathbf{k}\downarrow} \end{pmatrix}, \quad (1b)$$

where $a_{\mathbf{k}\sigma}$ or $b_{\mathbf{k}\sigma}$ are electron annihilation operators on two different orbits with momentum \mathbf{k} and spin $\sigma = \uparrow, \downarrow$.

$$H_d = \epsilon_d \sum_{\sigma} n_{d\sigma} + U_d n_{d\uparrow} n_{d\downarrow}, \quad (1c)$$

is the Hamiltonian for the Anderson impurity where ϵ_d is the impurity energy level and U_d is the interaction between electrons on the impurity. The interaction between the Anderson impurity d and the band electrons is described by $H_t + V$, where

$$H_t = V_d \sum_{\mathbf{k}, \sigma} \left(a_{\mathbf{k}\sigma}^\dagger d_\sigma + i b_{\mathbf{k}\sigma}^\dagger d_\sigma + \text{H.c.} \right) \quad (1d)$$

describes tunnelling of electrons between bulk bands and d -level and

$$V = V_0 \sum_{\alpha, \beta = a, b} \sum_{\mathbf{k}, \mathbf{k}', \sigma} \alpha_{\mathbf{k}\sigma}^\dagger \beta_{\mathbf{k}'\sigma}. \quad (1e)$$

where $V_0 \sim |V_d|^2 / D_0$ is an effective potential scattering between band-electrons induced by the d -level. D_0 is

the high-energy cut-off for the above Hamiltonian. We note that in usual analysis of Anderson impurity, the induced potential scattering term is neglected because it is irrelevant as far as Kondo physics is concerned. The situation is different here as we shall see in the following.

We start with diagonalizing $H_0 + V$. The eigenstates of H_0 alone is given by

$$H_0 = \sum_{\nu\sigma\mathbf{k}} \nu \varepsilon_{\mathbf{k}} \gamma_{\nu\mathbf{k}\sigma}^\dagger \gamma_{\nu\mathbf{k}\sigma}, \quad (2a)$$

where $\nu = \pm 1$ denotes the conduction and valence band.

$$\varepsilon_{\mathbf{k}} = \sqrt{M_k^2 + (\hbar v_F k)^2}, \quad (2b)$$

is the band dispersion where $M_k = mv_F^2 - B\hbar^2 k^2$. $\gamma_{\nu\mathbf{k}\sigma}$ are quasiparticle operators defined through the transformation,

$$\begin{aligned} a_{\mathbf{k}\sigma} &= e^{-i\alpha_{\mathbf{k}}/2} \left\{ \gamma_{c\mathbf{k}\sigma} \cos\left(\frac{\alpha_{\mathbf{k}}}{2}\right) + i\gamma_{v\mathbf{k}\sigma} \sin\left(\frac{\alpha_{\mathbf{k}}}{2}\right) \right\}, \\ b_{\mathbf{k}\sigma} &= e^{-i\alpha_{\mathbf{k}}/2} \left\{ \gamma_{c\mathbf{k}\sigma} \sin\left(\frac{\alpha_{\mathbf{k}}}{2}\right) - i\gamma_{v\mathbf{k}\sigma} \cos\left(\frac{\alpha_{\mathbf{k}}}{2}\right) \right\}, \end{aligned} \quad (2c)$$

where $\tan\left(\frac{\alpha_{\mathbf{k}}}{2}\right) = \sqrt{\frac{\varepsilon_{\mathbf{k}} - M_k}{\varepsilon_{\mathbf{k}} + M_k}}$. $\varepsilon_{\mathbf{k}}$ is gapped and the insulator is topological for $Bm > 0$. For $Bm > 1/2$ (assumed hereafter), the band dispersion has an "inverted-Mexican-hat" form (see Fig. 1) with dispersion minimum at a surface of nonzero wave-vector \mathbf{q} 's, with

$$\varepsilon_q = \frac{v_F^2}{2B} \sqrt{4Bm - 1}, \quad q = \frac{v_F}{\hbar B} \sqrt{Bm - \frac{1}{2}}, \quad (3)$$

where $q = |\mathbf{q}|$.

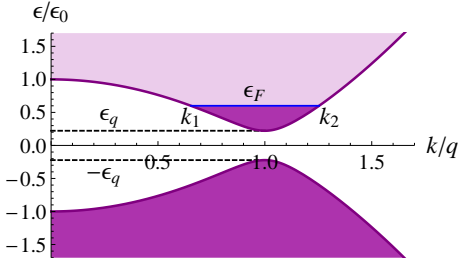


FIG. 1: Energy dispersion (2b) for $Bm = 20$. The dark (bright) regions denote the energy levels below (above) the Fermi energy ε_F . The band-edges occur at momentum q at energies $\pm\varepsilon_q$. (Here it is assumed that $\varepsilon_q < \varepsilon_F < mv_F^2$). k_1 and k_2 are two solutions of the equation $\varepsilon_{\mathbf{k}} = \varepsilon_F$.

The corresponding density of states (DOS) is

$$\rho(\varepsilon) = \Theta(|\varepsilon| - \varepsilon_q) \frac{\rho_0 |\varepsilon| g(\varepsilon)}{2\sqrt{\varepsilon^2 - \varepsilon_q^2}} \quad (4)$$

where $g(\varepsilon \gg \varepsilon_0) \sim \left(\frac{\varepsilon^2 - \varepsilon_q^2}{\varepsilon_0^2}\right)^{\frac{1}{4}}$, and $g(\varepsilon \rightarrow \varepsilon_q) \sim 2\left(\frac{\varepsilon_0^2 - \varepsilon_q^2}{\varepsilon_0^2}\right)^{\frac{1}{4}} = 2\sqrt{1 - \frac{1}{2Bm}}$. $\rho_0 = \frac{2v_F\sqrt{Bm}}{B^2\hbar^3}$ and $\varepsilon_0 = mv_F^2$. Notice that $\rho(\varepsilon)$ diverge at the band edge $\varepsilon \sim \pm\varepsilon_q$.

As was shown in Ref. [23], because of the diverging density of states at band-edge, an in-gap bound state (denoted by f) is induced for arbitrary weak scattering V_0 . The energy dispersion obtained after diagonalizing $H_0 + V$ has thus two parts: the bulk band structure described by Eq. (2) and an in-gap bound state described by an effective single-site Hamiltonian H_f ,

$$H_f = \sum_{\sigma} \epsilon_f f_{\sigma}^{\dagger} f_{\sigma} + U_f n_{f\uparrow} n_{f\downarrow}, \quad (5)$$

where $\epsilon_f \sim -\varepsilon_q + (V_0\rho_0)^2\varepsilon_q(1 - (2BM)^{-1})$ is located above the top of valence gap for repulsive V_0 . We have introduced an on-site Coulomb interaction U_f for this localized in-gap state. The tunnelling Hamiltonian H_t becomes in this new base $H_t \rightarrow \tilde{H}_t + H_{df}$, where

$$\tilde{H}_t = \tilde{V}_d \sum_{\mathbf{k},\nu,\sigma} \left(\gamma_{\nu\mathbf{k}\sigma}^{\dagger} d_{\sigma} + d_{\sigma}^{\dagger} \gamma_{\nu\mathbf{k}\sigma} \right), \quad (6)$$

describes tunnelling of band electrons to/from the d -level and

$$H_{df} = V_{df} \sum_{\sigma} (f_{\sigma}^{\dagger} d_{\sigma} + d_{\sigma}^{\dagger} f_{\sigma}) \quad (7)$$

describes tunnelling of electrons between d - and f -levels with $V_{df} \sim \sqrt{z}V_d$, where $z = \sum_{\mathbf{k},\nu} \langle 0 | \gamma_{\nu\mathbf{k}\sigma} f_{\sigma}^{\dagger} | 0 \rangle \sim V_0\varepsilon_q\rho_0^2(1 - (2BM)^{-1})$ and $\tilde{V}_d \sim V_d$. We have ignored the momentum dependence of \tilde{V}_d in writing down Eq. (6). The Hamiltonians $H_0 + H_d + H_f + H_t + H_{df}$ given through Eqs. (1c), (2), (5), (6), (7), define an effective two-impurities model $H_I^{(i)}$ describing the Anderson impurity. We note that although a particular model of 2DTI is employed in our derivation, the resulting model $H_I^{(i)}$ describes quite generally any insulator/semi-conductor with large density of states at the band edge such that an in-gap bound state is induced by the presence of the Anderson impurity.

Renormalization-Group Analysis

In the following we shall perform a renormalization-group (RG) analysis for $H_I^{(i)}$. To avoid confusion we first define various energy scales in our model. Unless otherwise specified, we shall assume $U_d \rightarrow \infty$ and

$$\epsilon_F - D_0 < \epsilon_d \ll \epsilon_f < \epsilon_F < 2\epsilon_f + U_f \ll \epsilon_F + D_0, \quad (8)$$

where ϵ_F is the Fermi energy (see figure 1). We shall integrate out the high energy degrees of freedom successively such that the bandwidth $D_0 \rightarrow D < D_0$ is reduced correspondingly.

We begin by analyzing the eigenstates of the effective impurity Hamiltonian $\bar{H}_I^{(i)} = H_d + H_f + H_{df}$ in the absence of band electrons. The eigenstates of $\bar{H}_I^{(i)}$ are specified by the configuration numbers (N_d, N_f) representing

the number of electrons on levels d and f . With energy scales specified by (8) the ground state has $N_d = N_f = 1$ and there are four possible states, a spin-singlet state $|S\rangle$ and three spin-triplet states $|T_m\rangle$ ($m = 0, \pm 1$). The singlet energy is modified when $V_{df} \neq 0$ while the triplet energy is unaffected.

Diagonalizing $\tilde{H}_I^{(i)}$, we obtain,

$$|S\rangle = \left\{ \frac{\alpha_S}{\sqrt{2}} (d_{\uparrow}^{\dagger} f_{\downarrow}^{\dagger} - d_{\downarrow}^{\dagger} f_{\uparrow}^{\dagger}) - \beta_f f_{\uparrow}^{\dagger} f_{\downarrow}^{\dagger} \right\} |0\rangle, \quad (9a)$$

with energy $\varepsilon_S = \epsilon_d + \epsilon_f - \frac{2V_{df}^2}{\Delta_f}$ and

$$\begin{aligned} |T_1\rangle &= d_{\uparrow}^{\dagger} f_{\uparrow}^{\dagger} |0\rangle, & |T_{-1}\rangle &= d_{\downarrow}^{\dagger} f_{\downarrow}^{\dagger} |0\rangle, \\ |T_0\rangle &= \frac{1}{\sqrt{2}} \{ d_{\uparrow}^{\dagger} f_{\downarrow}^{\dagger} + d_{\downarrow}^{\dagger} f_{\uparrow}^{\dagger} \} |0\rangle, \end{aligned} \quad (9b)$$

with energy $\varepsilon_T = \epsilon_d + \epsilon_f$, where $\alpha_S = \sqrt{1 - \beta_f^2}$, $\beta_f = \frac{\sqrt{2}V_{df}}{\Delta_f}$ and $\Delta_f = \epsilon_f - \epsilon_d + U_f$. We note that $\varepsilon_T > \varepsilon_S$, and the spin singlet state has lower energy.

The RG flow can be divided into several regimes: (i) $\epsilon_d > \epsilon_F - D > \epsilon_F - D_0$, in this regime charge fluctuations in both d and f states exist and there is no Kondo effect; (ii) $\epsilon_F - D > \epsilon_d$ but $\epsilon_f (\sim -\varepsilon_q) > \epsilon_F - D$ or $\epsilon_F + D > 2\epsilon_f + U_f$, in this regime the charge fluctuations on the d orbital is quenched but charge fluctuations still exist on the f orbital, the system is in the single Kondo impurity ($SU(2)$) regime; (iii) $\epsilon_F - D > \epsilon_f$ and $\epsilon_F + D < 2\epsilon_f + U_f$, in this regime charge fluctuations in both d and f states are quenched and the system is at the self-screened Kondo regime if $J_{df} > 0$ and in the $SO(3)$ Kondo regime if $J_{df} < 0$. Notice we require $U_f > \epsilon_F - 2\epsilon_f$ for this regime to exist. The RG analysis for the various regimes now follows:

Regime (i): Charge fluctuations on the d -orbital can be integrated out using a renormalization procedure proposed by Haldane a long time ago [28], but here the the spin-singlet and spin-triplet energies are, generically, renormalized separately. We note that in addition to renormalization of energies $\varepsilon_{S(T)}$ through \tilde{H}_t , the potential scattering term V and correspondingly ϵ_f and V_{df} are also renormalized. However the renormalization of V is weak and does not introduce any qualitative changes in general [28, 29]. Hence, for simplicity, we shall ignore the renormalization of V in the following. In this case the poor-man scaling procedure [28] results in the following scaling equation [31, 32] for $\varepsilon_{S(T)}$,

$$\frac{d\varepsilon_{S(T)}}{d \ln D} = V_{S(T)}^2 \rho(\varepsilon_F + D). \quad (10)$$

where $V_S^2 = \alpha_S^2 V_d^2$ and $V_T^2 = V_d^2$. The difference between V_S^2 and V_T^2 originates from the appearance of the renormalization factor α_S in the singlet state [see (9a)]. Notice

that $V_S^2 < V_T^2$ and the triplet energy level renormalizes faster than the singlet level. This opens the possibility that, as RG stops, the ground state of the system may become a triplet if the single-triplet level crossing occurs before the charge fluctuations in the d - and f -levels are quenched.

Solving Eq. (10), we find that the singlet-triplet energy spacing $J_{df}^{(i)}(D) = \varepsilon_T(D) - \varepsilon_S(D)$ is given by

$$\begin{aligned} J_{df}^{(i)}(D) &= \beta_f^2 \Delta_f \left(1 - \frac{V_d^2}{\Delta_f} \int_D^{D_0} \frac{dD'}{D'} \rho(\varepsilon_F + D') \right) \\ &\sim \beta_f^2 \Delta_f \left(1 - \frac{2V_d^2 \rho_0}{\Delta_f} \frac{\sqrt{D_0} - \sqrt{D}}{\sqrt{\varepsilon_0}} \right). \end{aligned} \quad (11)$$

where $D = D_i \sim \epsilon_F - \epsilon_d$ at the end of scaling.

Regime (ii): The charge fluctuation of the d -level is quenched at $D_i \sim \epsilon_F - \epsilon_d$ and we may perform a Schrieffer-Wolf transformation for the d -level, resulting in an effective Hamiltonian $H_I^{(ii)} = H_0 + H_f + H_{df} + H_K^{(ii)}$, where

$$H_K^{(ii)} = \frac{1}{2} \sum_{\alpha\beta=\gamma,f} J_{\alpha\beta} (\alpha_{\sigma}^{\dagger} \mathbf{s}_{\sigma\sigma'} \beta_{\sigma'}) \cdot \mathbf{S}_d, \quad (12)$$

where $\gamma_{\sigma} = \sum_{\nu, \mathbf{k}} \gamma_{\nu \mathbf{k} \sigma}$ describes band electrons, \mathbf{s} is the vector of Pauli matrices, \mathbf{S}_d is the localized spin of the d -level and

$$J_{\gamma\gamma} = \frac{2V_d^2}{\epsilon_F - \epsilon_d}, \quad J_{ff} = \frac{2V_{df}^2}{\epsilon_f - \epsilon_d}, \quad J_{\gamma f} = J_{f\gamma} = V_d V_f \left[\frac{1}{\epsilon_f - \epsilon_d} + \frac{1}{\epsilon_F - \epsilon_d} \right].$$

The Hamiltonian $H_K^{(ii)}$ describes coupling of the d -spin to γ and f electrons. Notice that charge fluctuations in the f -orbital is allowed in $H_K^{(ii)}$ through the mixed spin operator $\mathbf{S}_m = \frac{1}{2} (\gamma_{\sigma}^{\dagger} \mathbf{s}_{\sigma\sigma'} f_{\sigma'})$ and \mathbf{S}_m^{\dagger} . Fig. 2 clarifies the physics of the various interactions encoded in $H_K^{(ii)}$.

Charge fluctuations in the f -orbital can be integrated out gradually in regime (ii) with Anderson's poor-man scaling approach [29]. As a result, the exchange coupling constants $J_{\alpha\beta}$ are renormalized as,

$$\frac{dj_{\alpha\beta}}{d \ln D} = -j_{\alpha\gamma} j_{\gamma\beta} \frac{\rho(\varepsilon_F + D) + \rho(\varepsilon_F - D)}{2\rho_0}, \quad (13)$$

where $j_{\alpha\beta} = J_{\alpha\beta} \rho_0$. Defining

$$\mathcal{L}(D_f, D_i) = \int_{D_f}^{D_i} \frac{dD}{D} \frac{\rho(\varepsilon_F + D) + \rho(\varepsilon_F - D)}{\rho_0}, \quad (14)$$

we obtain

$$j_{\alpha\beta}(D) = j_{\alpha\beta}(D_i) + \frac{j_{\alpha\gamma}(D_i) j_{\gamma\beta}(D_i) \mathcal{L}(D, D_i)}{1 - j_{\gamma\gamma}(D_i) \mathcal{L}(D, D_i)}. \quad (15)$$

The scaling invariant, that is, the Kondo temperature $T_K^{(ii)}$, is obtained by solving the equation

$$j_{\gamma\gamma}(D_i) \mathcal{L}(T_K^{(ii)}, D_i) = 1, \quad (16)$$

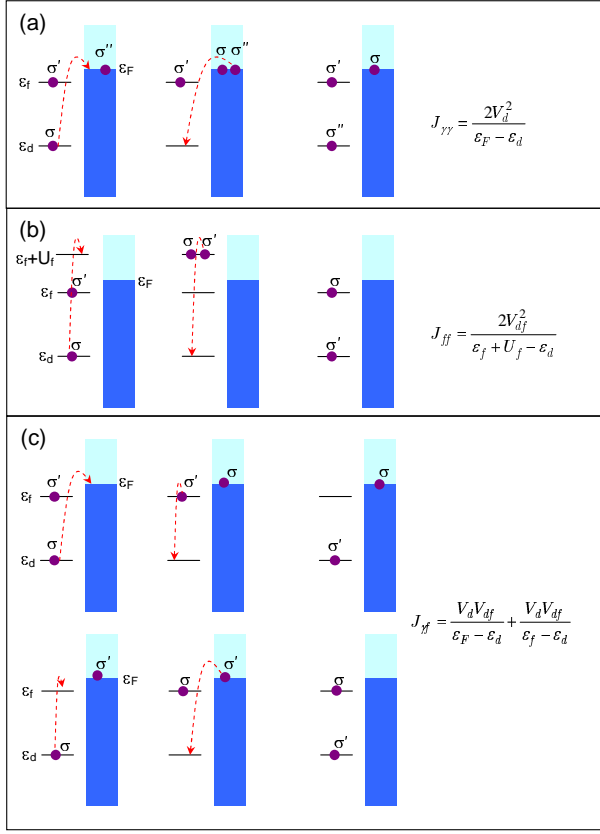


FIG. 2: Transitions induced by $H_K^{(ii)}$, Eq. (12) leading from an initial state on the left and ending at a final state on the right. The various processes are associated with exchange constants (a): $J_{\gamma\gamma}$, (b): J_{ff} and (c): $J_{\gamma f}$ and $J_{f\gamma}$

and scaling stops if $T_K^{(ii)} > D_{ii} = \min\{\epsilon_F - \epsilon_f, U_f - \epsilon_F + \epsilon_f\}$, indicating that the d -spin is quenched by the Kondo effect. This happens if (a) $\epsilon_F < -\epsilon_q$, in which case the d -spin is quenched by ordinary Kondo effect and the in-gap bound state becomes irrelevant; or (b) if $j_{\gamma\gamma}(D_i)$ is large enough. We note that $\mathcal{L}(D_{ii}, D_i)$ remains finite as long as $D_{ii} > 0$.

For $T_K^{(ii)} < D_{ii}$, scaling stops at $D = D_{ii}$. The effective coupling between f - and d -spins is a sum of contributions from H_{df} and $H_K^{(ii)}$, i.e.

$$J_{df} = J_{df}^{(i)}(D_i) + J_{ff}(D_{ii}).$$

and is ferromagnetic if $J_{df} < 0$. Assuming that $1 - j_{\gamma\gamma}(D_i)\mathcal{L}(D_{ii}, D_i)$ is of order $O(1)$, $\epsilon_F \sim \epsilon_q < \epsilon_0 \ll |\epsilon_d|$ and $U_f \leq |\epsilon_d|$, we find that $J_{ff}(D_{ii})$ is of the same order as $\beta_f^2 \Delta_f$ and $J_{df} < 0$ if $|V_d|^2 \geq \epsilon_0^{\frac{3}{2}} \sqrt{|\epsilon_d|}$.

Regime (iii): The scaling stops at regime (ii) with $D_{ii} \sim \epsilon_F + \epsilon_q$ if the chemical potential is located inside the band-gap which is the usual case for insulators. A more interesting scenario occurs if the chemical potential ϵ_F is located above the band-gap which may happen if the insulator is doped by impurities. Scaling continues in this

case where charge fluctuations in f -level is also quenched. In this case the mixed spin term \mathbf{S}_m becomes ineffective and we left with an effective Hamiltonian $H^{(2)} = H_0 + H_K^{(iii)}$, where

$$H_K^{(iii)} = J_K \mathbf{S}_\gamma \cdot \mathbf{S}_d + J_{df} \mathbf{S}_f \cdot \mathbf{S}_d. \quad (17)$$

where

$$\mathbf{S}_\gamma = \frac{1}{2} \sum_{\mathbf{k}\sigma, \mathbf{k}'\sigma', \nu} \left(\gamma_{\nu\mathbf{k}\sigma}^\dagger \mathbf{S}_{\sigma\sigma'} \gamma_{\nu\mathbf{k}'\sigma'} \right).$$

Here $J_K = J_{\gamma\gamma}(D_{ii}) = J_{\gamma\gamma}(D_i)/(1 - j_{\gamma\gamma}(D_i)\mathcal{L}(D_{ii}, D_i))$. Notice that $|J_{df}|$ is in general smaller than J_K by the renormalization factor z .

It is interesting to note that for $D_{ii} \gg |J_{df}|$, there exists a regime $D \gg |J_{df}|$ where the system is governed by the critical point between the $SO(3)$ - and the quenched-Kondo regimes which has $SO(4)$ symmetry [26]. In this regime the behavior of the system is governed by the $SO(4)$ critical point. The system crossovers to the low temperature $SO(3)$ - or self-screened-Kondo regime at $D < |J_{df}|$. We first consider the $SO(4)$ regime $D \gg |J_{df}|$. *$SO(4)$ Kondo fixed point:* In this case $J_{df} = 0$ and we may apply the Schrieffer-Wolf transformation directly to the spin-singlet and triplet states to obtain,

$$H_K^{SO(4)} = J_T (\mathbf{S} \cdot \mathbf{S}_\gamma) + J_{ST} (\mathbf{R} \cdot \mathbf{S}_\gamma) \quad (18)$$

where \mathbf{S} and \mathbf{R} are the ($S = 1$) spin operator and the Runge-Lenz operator, respectively with

$$\begin{aligned} S^+ &= \sqrt{2}(X^{10} + X^{0\bar{1}}), & S^- &= \sqrt{2}(X^{01} + X^{\bar{1}0}), \\ S^z &= X^{11} - X^{\bar{1}\bar{1}}, & \\ R^+ &= \sqrt{2}(X^{1S} - X^{S\bar{1}}), & R^- &= \sqrt{2}(X^{S1} - X^{\bar{S}\bar{1}}), \\ R^z &= -(X^{0S} + X^{S0}). & \end{aligned} \quad (19)$$

Here $X^{\lambda\lambda'} = |\lambda\rangle\langle\lambda'|$, $|\lambda(\lambda')\rangle = |S\rangle, |T_m\rangle$ ($m = 0, \pm 1$) are the spin singlet and triplet states. The coupling constants are given by $J_T = J_K/2$ and $J_{ST} = \alpha_S J_T$.

The scaling equations for the dimensionless couplings $j_\Lambda = J_\Lambda \rho_0$ are,

$$\begin{aligned} \frac{dj_T}{d \ln D} &= -(j_T^2 + j_{ST}^2) \frac{\rho(\epsilon_F + D) + \rho(\epsilon_F - D)}{2\rho_0}, \\ \frac{dj_{ST}}{d \ln D} &= -2j_T j_{ST} \frac{\rho(\epsilon_F + D) + \rho(\epsilon_F - D)}{2\rho_0}. \end{aligned} \quad (21)$$

The scaling equations can be solved by introducing coupling constants $j_n = j_T - (-1)^n j_{ST}$ [$n = 1, 2$]. It is easy to show that

$$j_n(D) = \frac{j_n(D_{ii})}{1 - j_n(D_{ii}) \mathcal{L}(D, D_{ii})}. \quad (22)$$

The couplings j_T and j_{ST} are then given by

$$j_{T(ST)}(D) = \frac{j_1(D) + (-)j_2(D)}{2}. \quad (23)$$

The scaling stops at the Kondo temperature T_{K_4} determined from the equation,

$$\left\{ j_T(\bar{D}_{ii}) + j_{ST}(\bar{D}_{ii}) \right\} \mathcal{L}(T_{K_4}, \bar{D}_{ii}) = 1 \quad (24)$$

if $T_{K_4} \gg |J_{df}|$. For $T_{K_4} < J_{df}$, the system flows to the $SO(3)$ fix point if $J_{df} < 0$. For $J_{df} > 0$, the two spins form a spin-singlet (self-screened Kondo effect) at $D \sim J_{df}$.

SO(3) Kondo fix point: When $J_{df} < 0$ and $T_{K_4} < |J_{df}|$, renormalization of j_{ST} stops at $D = D_{iii} \sim |J_{df}|$. For $D < D_{iii}$, the Kondo Hamiltonian becomes

$$H_K^{SO(3)} = J_T \mathbf{S} \cdot \mathbf{S}_\gamma. \quad (25)$$

The scaling equation for $j_T = J_T \rho_0$ is

$$\frac{dj_T}{d \ln D} = -j_T^2 \frac{\rho(\varepsilon_F + D) + \rho(\varepsilon_F - D)}{2\rho_0}, \quad (26)$$

with the usual solution

$$j_T(D) = \frac{j_T(D_{iii})}{1 - j_T(D_{iii})\mathcal{L}(D, D_{iii})}. \quad (27)$$

The scaling stops at the Kondo temperature T_{K_3} determined from the equation,

$$j_T(D_{iii}) \mathcal{L}(T_{K_3}, D_{iii}) = 1. \quad (28)$$

Resistivity and Impurity Magnetic Susceptibility

Having elaborated upon the theory in the weak coupling regime $T \gg T_K$'s we are now in a position to carry out perturbation calculations of experimental observables. In 3D, the most accessible ones are the impurity resistivity $R_{\text{imp}}(T)$ and the impurity magnetic susceptibility $\chi_{\text{imp}}(T)$. We shall be guided by the quest to find out how the special features of the TI's are reflected in these observables. These features are the occurrence of gap and the structure of the DOS especially near the band edges $\pm \varepsilon_q$. In addition, reducing the temperature results in the crossover between different scaling regimes of the couplings. Explicitly, there are three relevant temperature regimes denoted as $(ii), (iii), (iv)$ in order to match the notation of the corresponding scaling regimes discussed previously. The first regime, denoted as (ii) , is defined by $[D_i > T > D_{ii}]$ as given by equation (13) for scaling interval (ii) . Local moment behavior exists only at the d -level in this regime and therefore there is Kondo scattering with $SU(2)$ symmetry. The second regime, denoted as (iii) , is defined by equation (21) for scaling interval (iii) $[D_{ii} > T > D_{iii}]$. Here one may neglect the difference in energies between the singlet and triplet states and the system is at the $SO(4)$ Kondo regime; The third regime, denoted as (iv) , is defined by equation (26) for scaling interval (iv) $[D_{iii} > T > T_{K_3}]$. Here

there is Kondo scattering with $SO(3)$ symmetry (when $J_{df} < 0$) or the Kondo effect is screened if $J_{df} > 0$. The temperature dependence of the resistivity and magnetic susceptibility in these three different scaling regimes are distinct.

We assume that $\epsilon_F > \varepsilon_q$ (i.e. the TI is doped) and the system has a Fermi surface in the calculation of resistivity. The impurity resistivity as calculated in the framework of the ‘‘poor man’s scaling’’ formalism is given by,

$$R_{\text{imp}} = \frac{N_\nu R_0}{\mathcal{L}^2(T_{K_\nu}, T)}, \quad (29)$$

where $\nu = (ii), (iii), (iv)$, denotes the pertinent temperature regime as detailed above. The corresponding Kondo temperatures are $T_{K_{ii}}$ (16), $T_{K_{iii}} \equiv T_{K_4}$ (24) or $T_{K_{iv}} \equiv T_{K_3}$ (28), the numerical factors N_ν are, $N_{ii} = N_{iii} = 3/4$ and $N_{iv} = 2$. The constant R_0 is

$$R_0 = \frac{3\pi c_{\text{imp}}}{\hbar e^2 \rho_0^2} \frac{1}{v_1^2 + v_2^2}, \quad v_i \approx \frac{1}{\hbar} \left(\frac{\partial \varepsilon_{k_i}}{\partial k_i} \right),$$

where k_1 and k_2 are two solutions of the equation $\varepsilon_k = \epsilon_F$ (see Fig. 1).

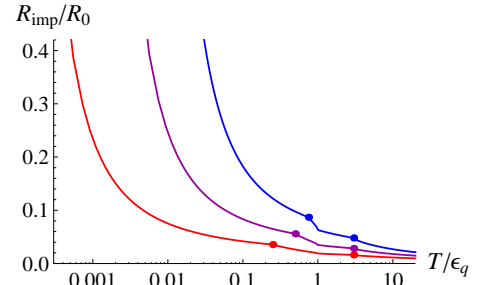


FIG. 3: Resistivity (29) as a function of temperature for $\epsilon_d = -80\varepsilon_q$, $\varepsilon_0 = 24\varepsilon_q$, $\epsilon_F = 2\varepsilon_q$ and different values of j : $j = 0.1$ [ref curve], $j = 0.12$ [purple curve] and $j = 0.14$ [blue curve]. The dots denote $T = D_{ii}$ and $T = D_{iii}$ separating the temperature intervals (ii) , (iii) and (iv) .

The resistivity as a function of the temperature is shown in Fig.3. It is seen that R_{imp} has different temperature dependence within the temperature intervals (ii) , (iii) and (iv) , with kinks observed at $T = D_{ii}$ and $T = D_{iii}$ [the points D_{ii} and D_{iii} are denoted by dots].

The Kondo scattering manifests itself also in the magnetic susceptibility [31]. The impurity susceptibility calculated in the framework of the ‘‘poor man’s scaling’’ is

$$\chi_{\text{imp}} = \frac{K_\nu \chi_0 T_{K_\nu}}{T} \left\{ P_\nu - \frac{1}{\mathcal{L}(T_{K_\nu}, T)} \right\}, \quad (30)$$

where $\chi_0 = 4c_{\text{imp}}\mu_B^2/T_{K_{ii}}$, $\nu = (ii), (iii), (iv)$, the Kondo temperatures are $T_{K_{ii}}$ (16), $T_{K_{iii}} \equiv T_{K_4}$ (24) or $T_{K_{iv}} \equiv T_{K_3}$ (28), $K_{ii} = K_{iii} = 1/4$, $K_{iv} = 2/3$, $P_{ii} = P_{iv} = 1$ and $P_{iii} = 2$.

The impurity magnetic susceptibility as a function of T is shown in Fig.4. The different temperature dependences

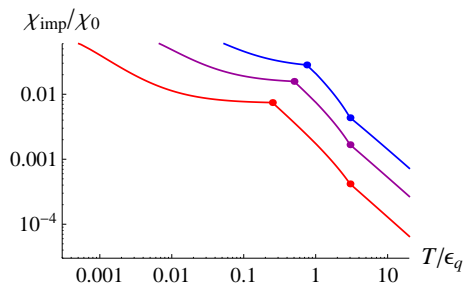


FIG. 4: Magnetic susceptibility (30) as a function of temperature for $\epsilon_d = -80\epsilon_q$, $\epsilon_0 = 24\epsilon_q$, $\epsilon_F = 2\epsilon_q$ and different values of j : $j = 0.1$ [ref curve], $j = 0.12$ [purple curve] and $j = 0.14$ [blue curve]. The dots denote $T = D_{ii}$ and $T = D_{iii}$ separating the temperature intervals (ii), (iii) and (iv).

of χ_{imp} at different temperature regimes (ii), (iii) and (iv) are obvious, with kinks observed at $T = D_{ii}$ and $T = D_{iii}$ [the points D_{ii} and D_{iii} are denoted by dots].

Summary

In this paper we analyze the interplay between the Anderson impurity and its induced in-gap bound state in a model of 2D topological insulator. Using a weak-coupling Renormalization Group (RG) analysis, we show that the exchange interaction J_{df} between the d - and induced f - spins may be renormalized dynamically to either positive or negative values. The parameters required to observe the above phenomena is not too restrictive ($|V_d|^2 \geq \epsilon_0^{\frac{2}{3}} \sqrt{|\epsilon_d|}$, $\epsilon_0 < U_f < U_d$) and is realistic. The system exhibits complex crossover behaviors at different parameter regimes as a result which can be observed in the temperature dependence of the impurity induced resistance and magnetic susceptibility. The crossover in the temperature dependence of both the resistivity and the impurity magnetic susceptibility at different regimes is a peculiar feature that can serve as an experimental confirmation of the above analysis.

We note that the physics described above is not limited to topological insulators but is a general consequence of (doped) insulators (and semi-conductors) with a large electronic density of states at the band edge such that in-gap bound states are easily induced by an Anderson impurity. Similar physics may be found in for example, two-layer graphene systems. Our paper is just a first step towards understanding the rich physics associated with impurities in these systems.

Acknowledgements

Discussions with C. M. Varma are highly appreciated. We acknowledge support by HKRGC through grant HKUST03/CRF09. The research of I.K and Y.A is partially supported by grant 400/12 of the Israeli Science

Foundation (ISF).

- [1] M. Z. Hasan and C. L. Kane, Rev. Mod. Phys. **82**, 3045 (2010).
- [2] X. L. Qi and S. C. Zhang, Rev. Mod. Phys. **83**, 1057 (2011).
- [3] J. E. Moore, Nature (London) **464**, 194 (2010).
- [4] H. Zhang, C. X. Liu, X. L. Qi, X. Dai, Z. Fang, and S. C. Zhang, Nat. Phys. **5**, 438 (2009).
- [5] Y. L. Chen et al., Science **325**, 178 (2009).
- [6] Y. Xia et al., Nat. Phys. **5**, 398 (2009).
- [7] C. Wu, B. A. Bernevig, and S. C. Zhang, Phys. Rev. Lett. **96**, 106401 (2006).
- [8] Joseph Maciejko, Chaoxing Liu, Yuval Oreg, Xiao-Liang Qi, Congjun Wu, and Shou-Cheng Zhang Phys. Rev. Lett. **102**, 256803 (2009).
- [9] Q. Liu, C. X. Liu, C. Xu, X. L. Qi, and S. C. Zhang, Phys. Rev. Lett. **102**, 156603 (2009).
- [10] R. R. Biswas and A. V. Balatsky, Phys. Rev. **B81**, 233405 (2010).
- [11] P. Roushan, J. Seo, C. V. Parker, Y. S. Hor, D. Hsieh, D. Qian, A. Richardella, M. Z. Hasan, R. J. Cava, and A. Yazdani, Nature **460**, 1106 (2009).
- [12] T. Zhang, P. Cheng, X. Chen, J. F. Jia, X. Ma, K. He, L. Wang, H. Zhang, X. Dai, Z. Fang, X. C. Xie, and Q. K. Xue, Phys. Rev. Lett. **103**, 266803 (2009).
- [13] Z. Alpichshev et al., Phys. Rev. Lett. **104**, 016401 (2010).
- [14] Z. Alpichshev, R. R. Biswas, A. V. Balatsky, J. G. Analytis, J. H. Chu, I. R. Fisher, and A. Kapitulnik, Rev. Lett. **108**, 206402 (2012).
- [15] A. M. Black-Schaffer and A. V. Balatsky, Phys. Rev. **B85**, 121103(R) (2012).
- [16] R. Zitko, Phys. Rev. B **81**, 241414 (2010).
- [17] M. T. Tran, and K. S. Kim, Phys. Rev. **B82**, 155142 (2010).
- [18] Q. Liu and T. X. Ma, Phys. Rev. **B80**, 115216 (2009).
- [19] W. Y. Shan, J. Lu, H. Z. Lu, and S. Q. Shen, Phys. Rev. **B84**, 035307 (2011).
- [20] J. Lu, W. Y. Shan, H. Z. Lu and S. Q. Shen, New J. Phys. **13**, 103016 (2011).
- [21] L. Andrew Wray, et al, Nat. Phys. **7**, 32 (2010).
- [22] X. Y. Feng, W. Q. Chen, J. H. Gao, Q. H. Wang, and F. C. Zhang, Phys. Rev. **B81**, 235411 (2010).
- [23] Cheung Chan and Tai-Kai Ng, Phys. Rev. **B85**, 115207 (2012).
- [24] Hai-Feng Lü, Hai-Zhou Lu, Shun-Qing Shen and Tai-Kai Ng, arXiv:1209.4710.
- [25] W.-Y. Shan, J. Lu, H.-Z. Lu and S.-Q. Shen, arXiv:1010.0503.
- [26] Y. Avishai, A. Golub and A. D. Zaikin, Phys. Rev. **B63**, 4515 (2001).
- [27] K. A. Kikoin, M. Kiselev and Y. Avishai, *Dynamical Symmetries for Nanostructures*, Springer (2011).
- [28] F.D.M. Haldane, Phys. Rev. Lett. **40**, 416 (1978).
- [29] P.W. Anderson, J. Phys. **C3**, 2346 (1970).
- [30] H.P. Paudel, M.N. Leuenberger, arXiv:1212.6772.
- [31] A.C. Hewson, *The Kondo Problem to Heavy Fermions*, (Cambridge University Press, 1993).
- [32] K. Kikoin and Y. Avishai, Phys. Rev. B **65**, 115329 (2002).